

Surface Morphology and Sensing Property of NiO-WO₃ Thin Films Prepared by Thermal Evaporation

Dong-myong Na ¹, L. Satyanarayana ², Gwang-Pyo Choi ³, Yong-Jin Shin ⁴
and Jin Seong Park ^{1,*}

¹ Department of Advanced Materials and Engineering, Chosun University, Gwangju 501-759, Korea.

² Research Institute of Energy Resources Technology, Chosun University, Gwangju 501-759, Korea.

³ JAMIC, Sunchun, Jeonnam 540-856, Korea

⁴ Department of Physics, Chosun University, Gwangju 501-759, Korea

*Author to whom correspondence address should be addressed: jsepark@chosun.ac.kr

Received: 18 November 2005 / Accepted 30 November 2005 / Published: 1 December 2005

Abstract: WO₃ and NiO-WO₃ thin films of various thicknesses were deposited on an Al₂O₃-Si (alumina-silicon) substrate using high vacuum thermal evaporation. After annealing at 500°C for 30 minutes in air, the crystallinity and surface morphology of WO₃ and NiO-WO₃ thin films were investigated using X-ray diffraction (XRD) and Scanning Electron Microscopy (SEM). It is observed that the WO₃ thin films were resulted in cracks between the polycrystalline grains and the grain growth was increased with increasing thickness causing deteriorated sensing characteristics of the films. On the other hand, an optimum deposition of NiO on WO₃ thin film has inhibited the grain growth and improved the sensitivity of the films. The inhibition is limited to a certain thickness of WO₃ and NiO content (mol %) of inclusion and below or above this limitation the grain growth could not be suppressed. Moreover, the deposition sequence of NiO and WO₃ is also playing a significant role in controlling the grain growth. A probable mechanism for the control of grain growth and improving the sensing property has been discussed.

Keywords: Tungston Oxide, Thin films, Thermal evaporation, surface morphology

1. Introduction

Metal oxide thin films have become the focus of many studies in recent years in view of their electrical properties, stability at high temperature and durability. Many researchers have studied metal oxide thin films as electronic materials due to their structural simplicity and low cost [1]. However, in order to improve such devices the surface defects and the characteristics of thin films prevailing in film fabrication processes need to be carefully understood.

WO₃ as a wide band gap n-type semiconductor was considered to be the best candidate in its thin film form and attracted much interest as conductance type gas sensor especially to detect H₂S, NO_x, and organophosphate compounds [2, 3]. The sensitivity of the WO₃ thin films is known to be improved by the accurate control of film microstructure and stoichiometry [4-7]. WO₃ thin films used as sensing materials are typically amorphous or polycrystalline, and are usually treated by post deposited annealing [8]. The effect of annealing causes stoichiometry or microstructural changes that typically lead to a decrease in film conductivity [9]. In our earlier studies we have reported the microstructure control and electrical properties of thick film WO₃ as a function of NiO doping, partial pressure of oxygen and concentration of NO₂ [10]. In this paper, we report the surface characteristics of WO₃ and NiO-WO₃ thin films deposited by thermal evaporation and their growing mechanism as a function of amount of NiO (mol%) and WO₃ thin film thickness in order to control the surface morphology and microstructure and to improve the sensing property.

2. Experimental

WO₃ and NiO-WO₃ thin films were deposited on an n-type silicon (100) single crystal substrate by high vacuum thermal evaporation. Al₂O₃ was deposited about 200nm thickness as an insulation layer between the substrate and WO₃ films by electron-beam evaporator. During deposition, 3 sccm of oxygen flow rate at 7.23 KW of E-beam power and 70 mA of electric current was maintained. And a base pressure of 2.3x10⁻⁵ Torr and working pressure of 1.7x10⁻⁴ Torr was applied. The voltages of WO₃ and NiO were maintained at 3.0 V and 4.5 V and the chamber vacuum was 5x10⁻⁵ Torr. WO₃ (Aldrich, 99.99%) and NiO (Kanto chemical, 99.99%) powders were used as deposition materials. To measure the sensing property, two Au electrodes were designed 1mm apart from each other and were printed on Al₂O₃/Si-substrate by screen printing method.

Fig. 1 illustrates the deposition scheme of WO₃ and NiO-WO₃ thin films. Different weights of WO₃ powders (0.25, 0.5, 0.75 and 1.0g) were deposited onto the Al₂O₃-Si substrates and consequently obtained respective 100, 120, 150 and 200nm thickness WO₃ films. Initially, a fixed amount of NiO (0.0009g or 0.33mol%) was deposited onto the different thickness WO₃ thin films. Further, various mol% of NiO was deposited on a fixed 0.75 g or 150nm thickness WO₃ film. Finally, the sequence of deposition process of WO₃ and NiO was altered and studied based on the surface morphology of the thin films. Following the deposition, all the films were annealed at 500°C for 30 minutes in air in order to improve the layer crystallinity.

The crystallinity and crystal structure of the films was analyzed by X-ray diffraction (Rigaku, D/Max-3C, CuK=1.5405Å) and the microstructure of the films was investigated by Scanning electron microscopy (FE-SEM- Hitachi S-4700).

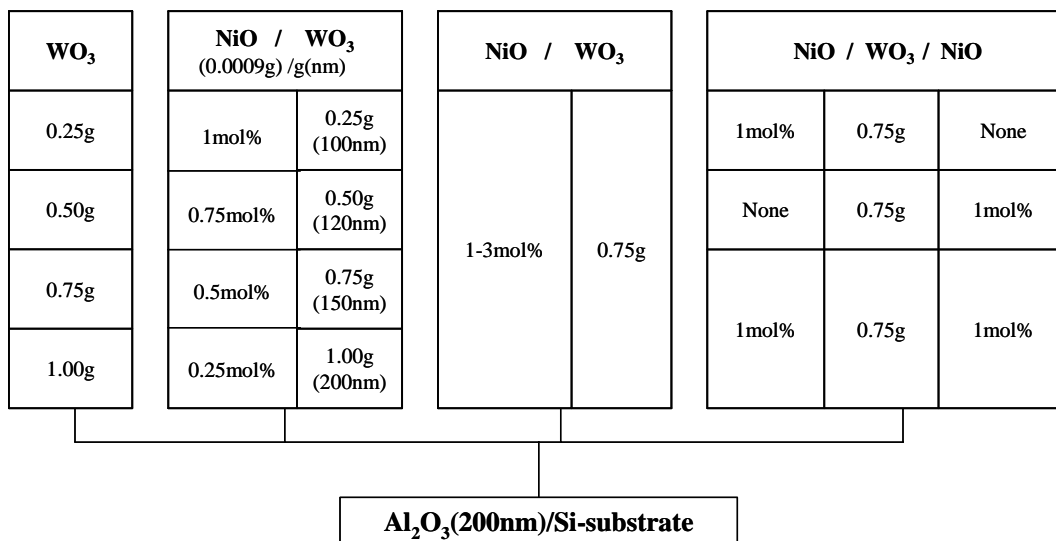


Figure 1. Specimen preparation processes of WO₃ and NiO-WO₃ thin films.

3. Results and discussion

Fig. 2 (a) and (b) shows the X-ray diffraction pattern of various thickness deposited WO₃ thin films before and after heat treatment at 500°C for 30minuts in air. Regardless of thickness, the as-deposited WO₃ thin films were existed in an amorphous phase and no other peaks except a Si(100) peak at 33°(2θ) and a broad peak between 20-30° (2θ) were observed. After annealing, WO₃ phase was grown into polycrystalline with increasing intensity, indicating a major peak (200) and other minor peaks in various directions. The obtained XRD peaks were in accordance with JCPDS data card No.83-0951 of WO₃. Similar results of XRD were obtained when different mol% of NiO was deposited onto the WO₃ films. It was difficult to distinguish NiO-WO₃ thin film structure except the (002) peak tended stronger. The NiO phase was not detected by XRD since the amount of NiO is less and below the detection limit of the instrument.

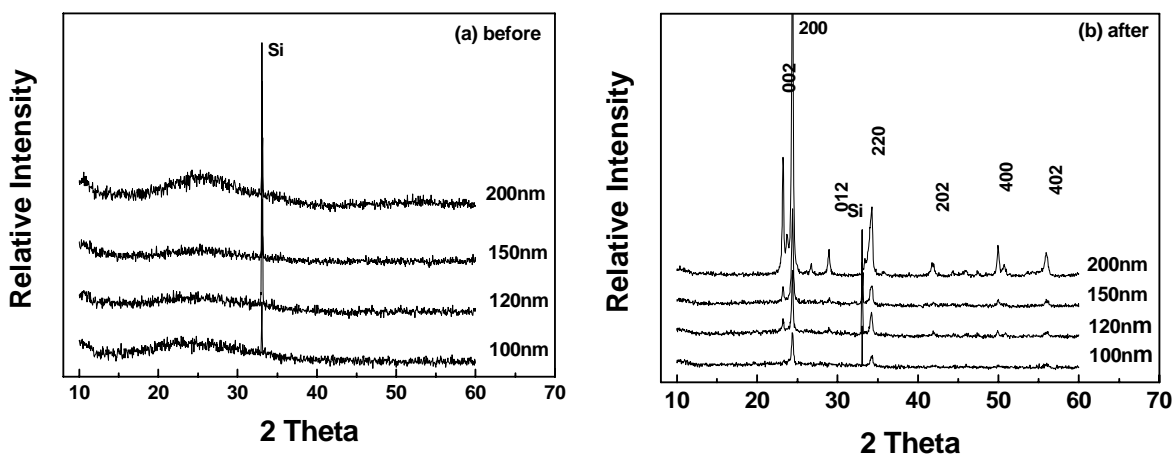


Figure 2. XRD patterns of WO₃ films (a) before and (b) after annealing at 500°C for 30 minutes.

Fig. 3 shows the variation of XRD peak intensities as a function of thickness for pure WO₃ films after annealing. The major peak intensities were almost equal up to 150 nm WO₃ thickness, however, between 150-200 nm thickness the intensities of (220), (200) and (002) peaks were steeply increased. Similar effect was observed after NiO addition also.

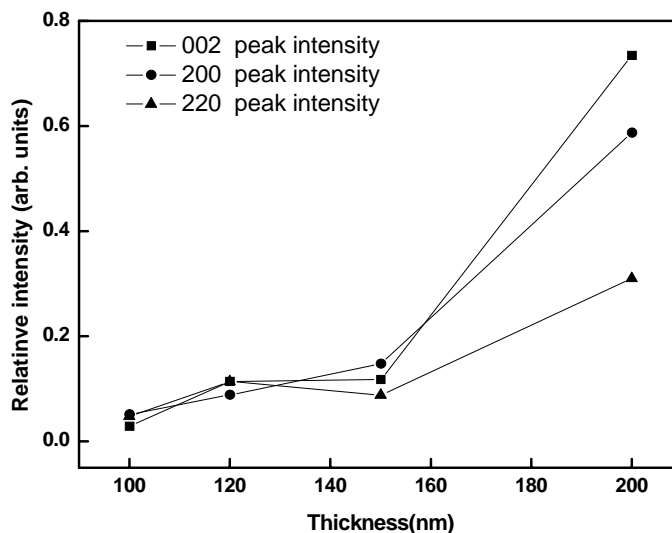


Figure 3. Variation of XRD peak intensities as a function of WO₃ film thickness.

Fig. 4 shows the variation of peaks intensity as a function of NiO addition (mol%) on 150nm WO₃ film. Though there was no major change observed in peak intensities up to 2 mol% NiO addition, the intensity of (002) major peak was steeply increased with above 2 mol% of NiO addition, remaining the intensities of other peaks unchanged. The sudden increase in the peak intensity indicates a change in microstructure and film properties. The change in relative intensity was calculated as the ratio of the particular peak intensity to the sum of all intensities of the film according to equation (1).

$$I_T = I_{hkl} / \sum I_{hkl} \quad (1)$$

Fig. 5 shows the SEM micrographs of surface morphology and cross section of WO₃ thin films deposited for (a) 100 (b) 120 (c) 150 and (d) 200 nm thickness after annealing. The surface morphology is generally similar except with increased thickness. The average grain size of these films is about 0.5 μm. However, large polycrystalline grains were formed by the necking or merging of small grains during the annealing process. The cracks between the large grains could be formed as the small grains became closer and agglomerated at the annealing temperature, and got shrinkage while undergoing the cooling process. Large grains or crack gaps cause to decrease the surface area and connectivity of films and to deteriorate film properties of electronic materials. It can be observed that crack gaps were increased with increasing film thickness.

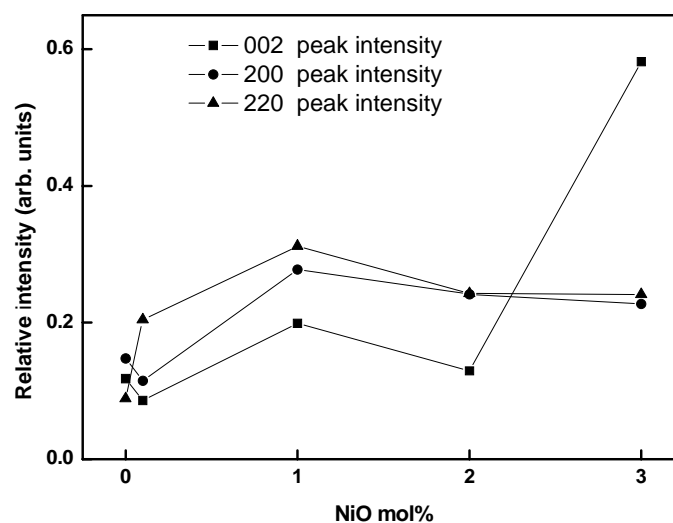


Figure 4. XRD peak intensity variation as a function of NiO content (mol%) on 150nm WO₃ thin film.

The grain growth was effectively inhibited by depositing NiO on WO₃ thin film surfaces. Fig. 6 (a-d) shows the surface morphology after a fixed amount of NiO (0.0009g, equivalent to 1.0, 0.75, 0.5 and 0.25 mol%) was deposited onto the respective films of 100, 120, 150 and 200nm (0.25, 0.5, 0.75, 1.0g weight) WO₃ films. NiO deposition was found to be inhibited the grain growth in only 100 and 120 nm films (a, b), but not in 150 and 200nm WO₃ films (c, d) as observed in the figure. Moreover, the crack gap was increased with WO₃ thickness above 120nm. It means that 1.0-0.75mol% NiO addition could effectively able to control the surface cracks of 100-120nm thickness WO₃ films, and below or above this critical range of NiO and WO₃ thickness, surface cracks were not inhibited as seen in Figs. 6 (c) and (d). Thus, this is one limitation of inhibition of grain growth in NiO deposited WO₃ thin films.

Similarly, by fixing WO₃ thickness, NiO content was varied. 1-3 mol% of NiO was deposited on 150nm WO₃ thin films and observed SEM surface morphologies as in Fig. 7 (a-c). It is observed that 1-2 mol% NiO added films contain small and uniform grain size (Fig. a, b) but 3 mol% NiO added surface (Fig. c) depicts indistinct large grains. This is because, 1-2 mol% NiO is forming small island like structures penetrating the inter-granules of WO₃ and suppress the formation of large grains. But in case of 3mol%, NiO is becoming excess and forming like a thin continuous layer over WO₃ surface and could not penetrate into the inter-granules of WO₃.

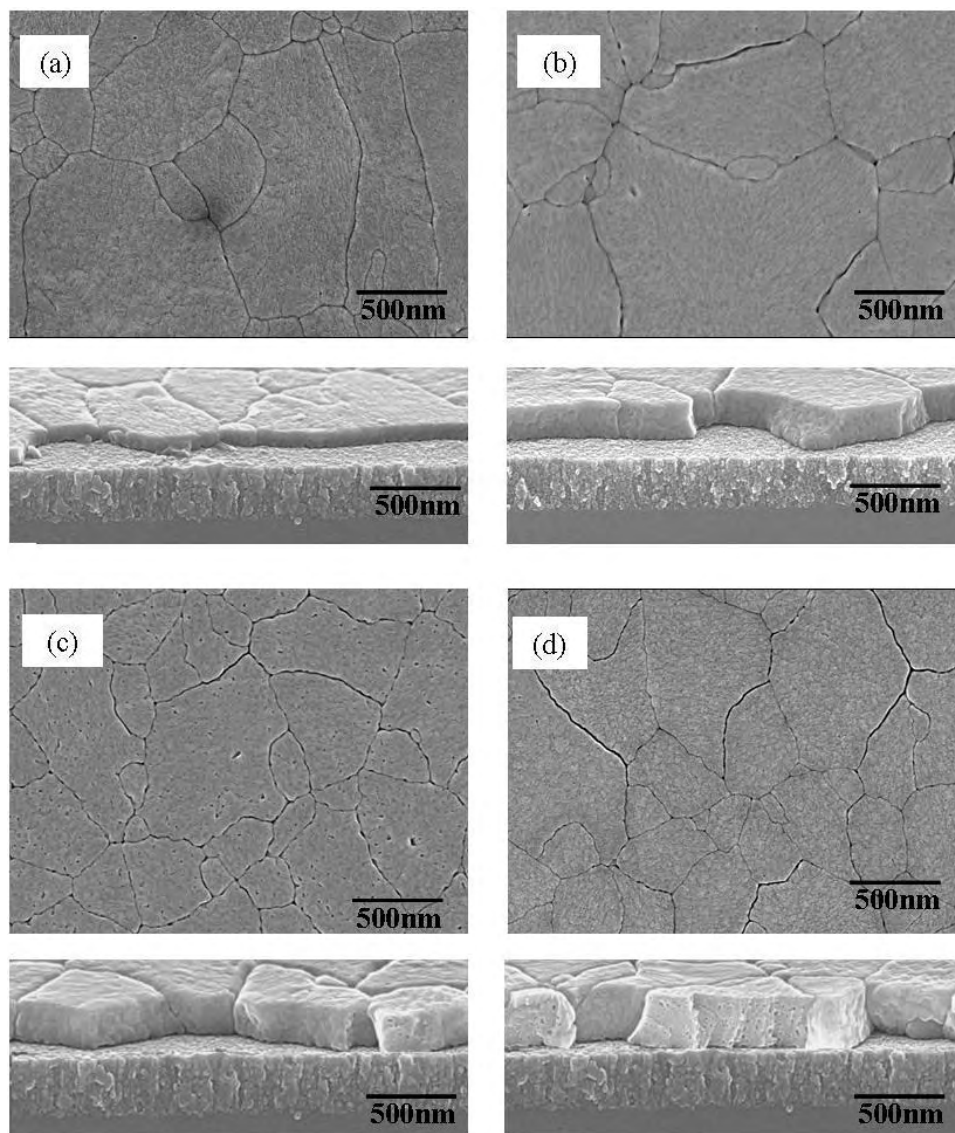


Figure 5. SEM micrographs of surface morphology and cross section of WO_3 thin films. (a) 100 (b) 120 (c) 150 (d) 200nm thicknesses after annealing.

It can be deduced from the above two results that, the grain growth was not inhibited in 150nm thickness WO_3 films if the content of NiO is less than 0.75 mol% and more than 2 mol% as seen in Figs. 6(c) and Fig. 7 (c). It can only be controlled if the addition of NiO is between 1-2 mol% as shown in Fig. 7(a) and (b). Hence, the inhibition is limited to a certain thickness of WO_3 (100-150 nm) and NiO content (0.75-2 mol%) of inclusion, and below or above this limitation the cracks could not be suppressed. This inference is in quite coincidence with the XRD peak intensity patterns observed in Fig.3 and Fig.4.

Further, the deposition sequence of NiO on WO_3 is also having an effect on the surface properties as shown in Fig. 8. The deposition of NiO beneath WO_3 film (Fig.8a) could not inhibit any grain growth. Whereas NiO deposition on both sides of the WO_3 film (Fig.8b) could control the cracks to some extent by forming island like structures on WO_3 surface as observed from the figure. Hence, it can be implied that an optimum NiO deposition above WO_3 film is only the most effective process to suppress the grain growth of WO_3 films.

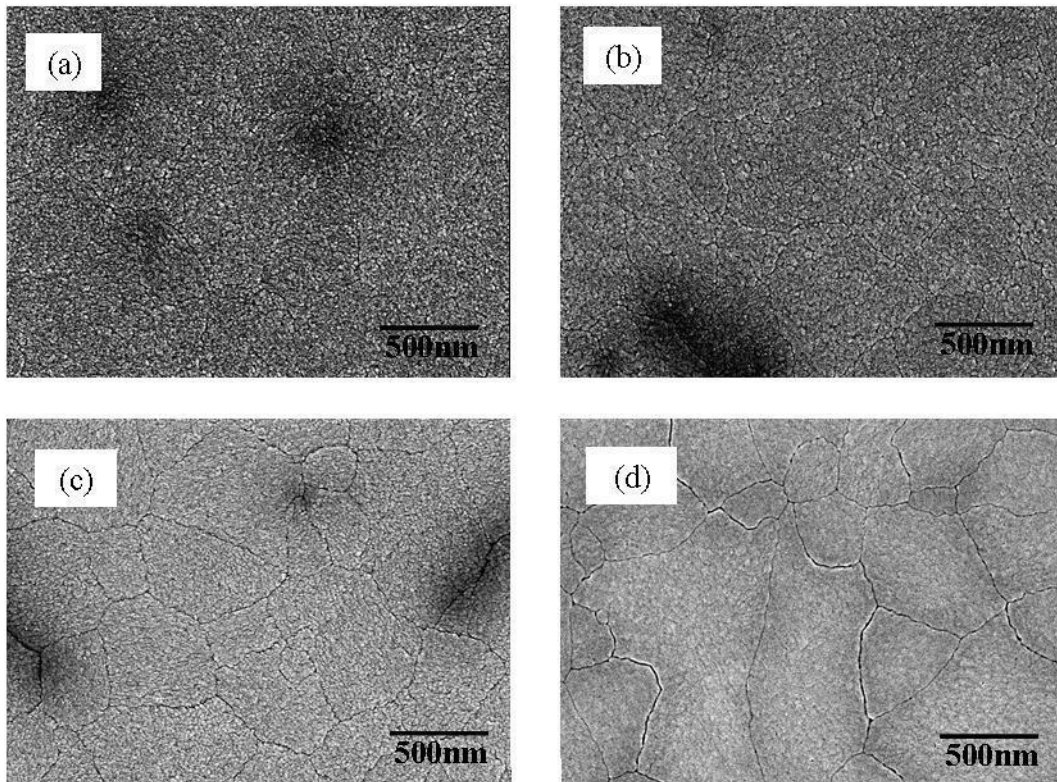


Figure 6. SEM micrographs of NiO:WO₃ surfaces of (a) 100nmWO₃:1mol%NiO (b) 120nmWO₃:0.75mol%NiO (c) 150nmWO₃:0.5mol%NiO (d) 200nmWO₃:0.25mol%NiO films.

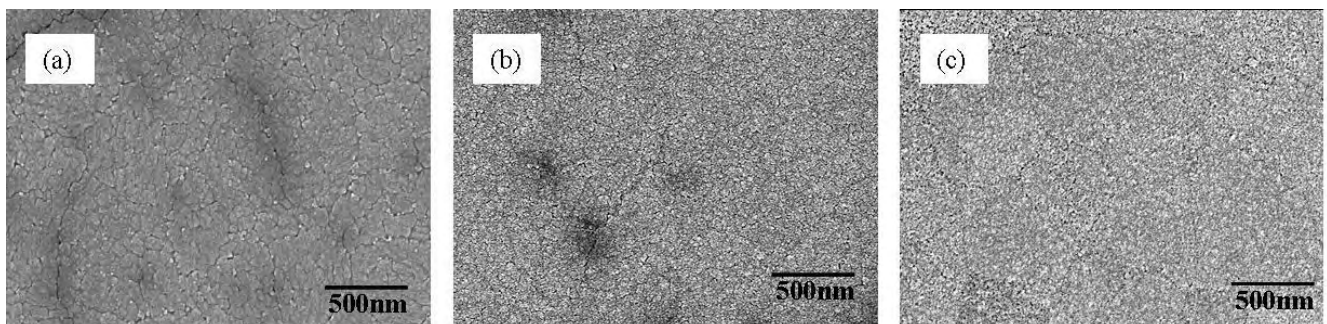


Figure 7. SEM micrographs of 150nm WO₃ films after deposition of (a) 1 (b) 2 (c) 3 mol% NiO.

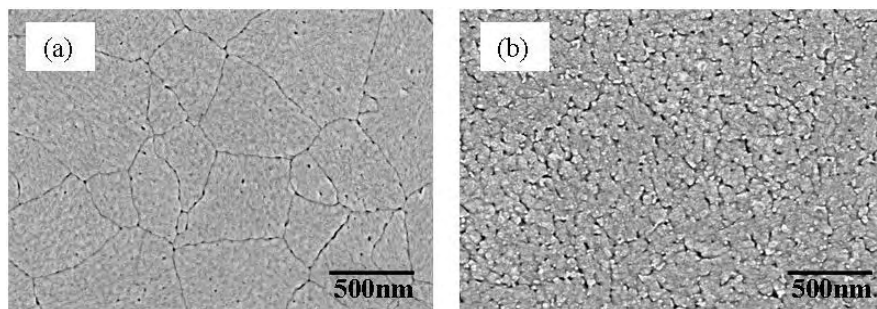


Figure 8. SEM micrographs showing deposition sequence of NiO:150nm WO_3 films. (a) NiO beneath WO_3 , (b) NiO on both sides of WO_3 .

The mechanism involved in inhibition of grain growths by deposition of NiO on the WO_3 thin film surface is illustrated in Fig. 9. During normal course of annealing large grains will be forming on WO_3 surface due to material diffusion and merging effects. However, less amount of NiO deposition can not control the grain growth as they are widely dispersed and insufficient on WO_3 surface (Fig. a). Similarly, excess amount of NiO leads to the formation of a thin continuous layer over WO_3 surface leaving them uncontrolled underneath (Fig. c). But an optimum amount of NiO in proportion to the WO_3 film thickness could only suppress the grain growth by interfering into the inter-granules with sufficient NiO- WO_3 correlation (Fig. b).

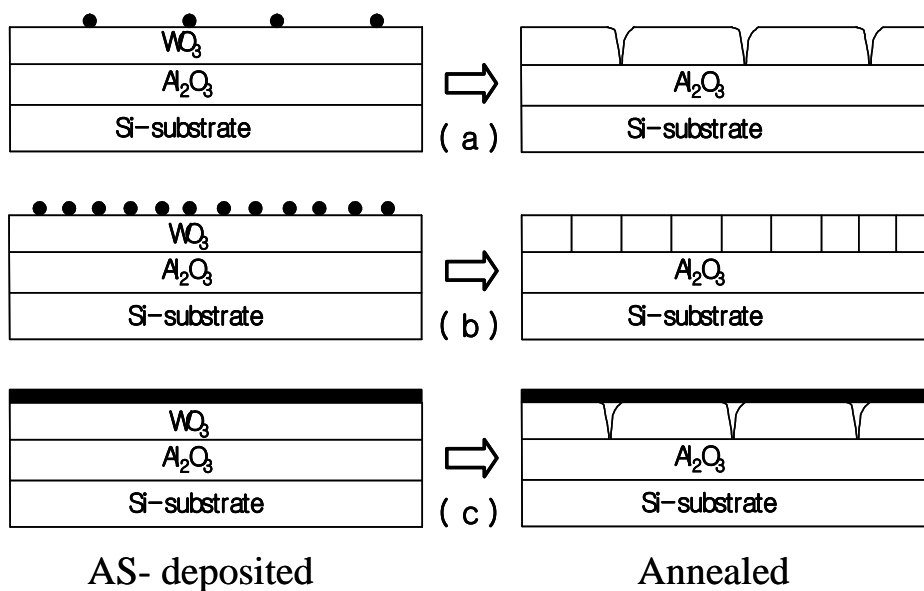


Figure 9. Mechanism of the crack formation and suppression in NiO deposited WO_3 films with (a) less (b) optimum (c) excess of NiO. Black dots and layers represent NiO.

WO_3 thin films were found to be one of the best candidates to detect NO_x gas. However, the sensitivity to NO_x gas was comparatively not so high. Fig. 10 shows the change in resistances with time when 5 ppm NO_2 gas was passed onto the various surface of (a) pure WO_3 (150nm) (b) NiO(1mol%): WO_3 (150nm) (c) NiO(0.5mol%): WO_3 (150nm) and (d) NiO(3mol%): WO_3 (150nm) thin films. 150nm pure WO_3 thin film was able to detect a change of 40×10^6 ohms in resistance at $250^\circ C$

operating temperature. Whereas NiO(1mol%) deposited WO_3 thin film has shown a change more than that of one order of the pure WO_3 film at the same NO_2 concentration. This reflects the improvement in sensitivity of the 1 mol % NiO: WO_3 thin film as NO_2 sensor. On the other hand, the fast response and recovery characteristics of the sensor were also be observed from Fig. 10 (b).

Similarly, the change of resistance of the NO_2 sensor when the NiO addition is less or more of the critical limit was depicted in Fig. 10 (c) and (d). In both the cases the sensing property was much deteriorated due to the surface defects as compared to that of Fig. 10 (b).

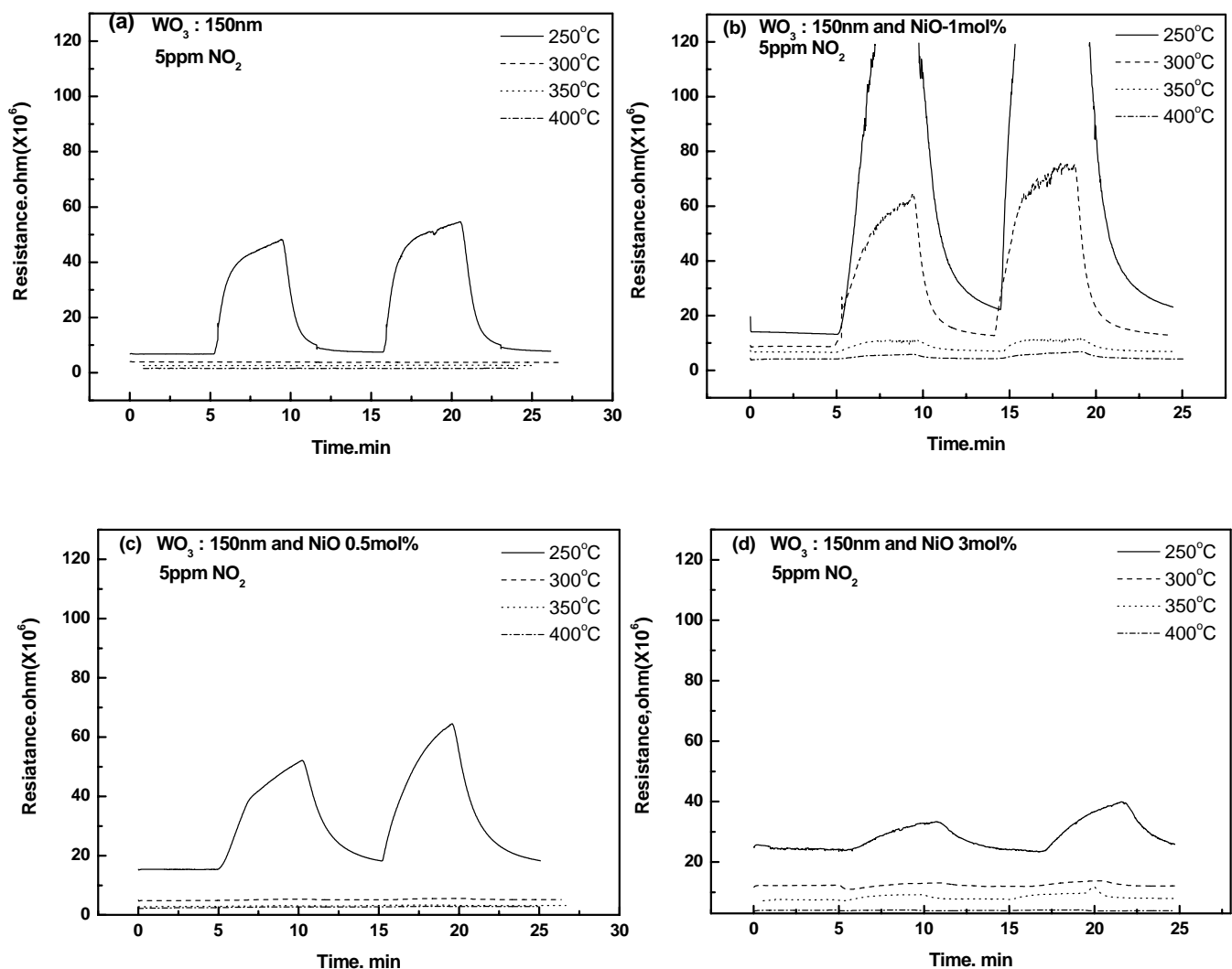


Figure 10. Change of resistance to 5 ppm NO_2 gas with time. (a) 150nm pure WO_3 . (b) NiO(1mol%): WO_3 (150nm) (c) NiO (0.5mol%): WO_3 (150nm) (d) NiO(3mol%): WO_3 (150nm) thin film.

4. Conclusions

WO_3 and NiO- WO_3 thin films of various thickness and sequence were deposited on n-type Si(001) substrate by high vacuum thermal evaporation. Al_2O_3 was deposited on silicon as an insulation layer

between substrate and thin film by e-beam evaporation. After annealing at 500°C for 30 minutes in air, the amorphous thin films were grown into large polycrystalline grains along with formation of cracks between them. An optimum deposition of NiO on WO₃ thin films has inhibited the grain growth in the films. The inhibition is limited to a certain thickness of WO₃ and NiO content (mol%) of inclusion and below or above this limitation the cracks were not suppressed. Similarly, when NiO is deposited beneath or both sides of WO₃ surface it could not control the grain growth effectively, whereas when deposited above of the WO₃ surface it could sufficiently control the grain growth. The suppression of the grain growth in the WO₃ thin films has lead to the improved surface morphology and NO_x sensing properties.

Acknowledgements

This work was supported by Korea Research Foundation Grant (KRF-2004-005-D00008).

References

1. Papadopoulos, C. A.; Vlachos, D. S.; Avaritsiotis, J. N. Comparative study of various metal oxide based gas sensor architectures. *Sensors and Actuators B* **1996**, *32*, 61-69.
2. Cantalini, C.; Pelino, M.; Sun, H. T.; Faccio, M.; Santucci, S.; Lozzi, L.; Passacantando, M. Cross-sensitivity and stability of NO₂ sensors from WO₃ films. *Sensors and Actuators B* **1996**, *35-36*, 112-118.
3. Penza, M.; Tegliente, M. A.; Merenghi, L.; Gerardi, C.; Martucci, C.; Cassano, G. Tungsten oxide (WO₃) sputtered thin films for a NO_x gas sensor. *Sensors and Actuators B* **1998**, *50*, 9-18.
4. Antonik, M. D.; Schneider, J. E.; Wittman, E. L.; Snow, K.; Lad, R. J. Micro structural effects in WO₃ gas sensing films. *Thin Solid Films* **1995**, *256*, 247-252.
5. Sun, H. T.; Cantalini, C.; Lozzi, L.; Passacantando, M.; Santucci, S.; Pelino, M. Micro structural effect on NO₂ sensitivity of WO₃ thin film gas sensors. Part 1. Thin film devices, Sensors and Actuators. *Thin Solid Films* **1996**, *287*, 258-265.
6. Manno, D.; Serra, A.; Di Giulio, M.; Micocci, G.; Tepore, A. Physical and structural characterization of tungsten oxide thin films for NO gas detection, *Thin Solid Films*, **1998**, *324*, 44-51.
7. Dwyer, D. J. Surface chemistry of gas sensors: H₂S on WO₃ films. *Sensors and Actuators B* **1991**, *5*, 155-159.
8. Fruhberger, B.; Grunze, M.; Dwyer, D. J. Surface chemistry of H₂S sensitive tungsten oxide films. *Sensors and Actuators B* **1996**, *31*, 167-174.
9. Xu, Z.; Vetelino, J. F.; Lee, R.; Parker, D. C. Electrical properties of tungsten trioxide films. *J. Vac. Sci. Technol. A* **1990**, *8*, 3634-3638.
10. Noh, W. S.; Shin, Y.; Kim, J.; Lee, W. S.; Hong, K.; Akbar, S. A.; Park, J. S. Effects of NiO addition in WO₃-based gas sensors prepared by thick film process. *Solid State Ionics* **2002**, *152-153*, 827-832.